Available online at www.sciencedirect.com
ScienceDirect
Procedia CIRP 46 (2016) 631 – 635
www.elsevier.com/locate/procedia

7th HPC 2016 – CIRP Conference on High Performance Cutting

Approach of characterization of the grinding wheel topography as a contribution to the energy modelling of grinding processes

Fritz Klocke[a], Christian Wrobel[a,*], Matthias Rasim[a], Patrick Mattfeld[a]

[a]*Laboratory for Machine Tools and Production Engineering (WZL), RWTH Aachen University, Steinbachstrasse 19, 52074 Aachen, Germany*

* Corresponding author. Tel.: +49-241-80-28186; fax: +49-241-80-22293. *E-mail address:* c.wrobel@wzl.rwth-aachen.de

Abstract

A major percentage of the kinematic energy during the grinding process is converted into heat. The energy conversion is significantly influenced by the grinding wheel topography. Therefore the distribution and the shape of the cutting edges have to be considered in order to give a general model of energy conversion in grinding. This paper introduces an approach to describe and characterize the cutting edges of a grinding wheel topography, taking the elasto-plastic material behavior of the workpiece into account. Finally, based on experimental results the influence of the grinding wheel topography on energy conversion is shown using the presented model.

Peer-review under responsibility of the International Scientific Committee of 7th HPC 2016 in the person of the Conference Chair Prof. Matthias Putz

Keywords: Grinding; Energy; Modelling; Topography

1. Introduction

In the machining of a variety of components the grinding process stays at the end of the process chain. During grinding most of the applied energy is converted into heat. The resulting temperature has a significant influence on the process results [1]. Thus, a precise knowledge of the resulting energy conversion in the process is necessary for an application-oriented design and optimization of grinding processes.

In the past the energy conversion in grinding processes was investigated in numerous scientific studies and the findings were transferred into a variety of models. Basically, the existing approaches are related to pure kinematic-empirical relationships [1] or attributed to the modelling approaches of Shaw or Malkin [2,3]. For the last model approach, Ghosh and Singh have presented the most detailed model up to now [4,5]. The influence of the shape of the cutting edges on the energy conversion is considered, if at all, by one-dimensional, often averaged, parameters such as the rake angle [6,7,8] or the cutting edge radius [9]. The statistical grain distribution of a grinding wheel topography is only considered in a few works through significantly simplified modelling approaches [10,11].

Thus, there is no direct consideration of the grinding wheel topography in the existing models. Consequently, the distribution and the shape of the cutting edges are neglected. As a result, the existing models are only valid for a grinding wheel in its present topography state. If the grinding wheel topography changes by a dressing process, wear or a change of the grinding wheel specification, a new parameterization of the energy model by means of empirical studies is necessary.

In order to give a general modeling of energy conversion in grinding processes, the grinding wheel topography engaging with the workpiece has to be considered. This paper presents a kinematic-geometric engagement model, which allows determining and geometrical analyzing the shape of the cutting edges of a measured topography. Furthermore, based on experimental results, the influence of the cutting edges' shape on the energy conversion is shown and discussed using the developed model.

Peer-review under responsibility of the International Scientific Committee of 7th HPC 2016 in the person of the Conference Chair Prof. Matthias Putz
doi:10.1016/j.procir.2016.04.011

2. Kinematic-geometric engagement model

The developed kinematic-geometric engagement model determines and geometrical analyses the shape of the cutting edges of a grinding wheel topography.

First, the measurement procedure of the grinding wheel topographies is introduced. Since the developed approach uses an iterative calculation approach first the cutting edge characteristics as well as their calculation using the topography measurement plots is presented. Based on this, the developed kinematic-geometric engagement model is described, which identifies the kinematic cutting edges taking the elasto-plastic material behavior of the workpiece into account. Finally, the experimental results of three investigated single-layered, electroplated CBN grinding wheels are presented and discussed.

2.1. Measurement of the grinding wheel topography

The measurement of the grinding wheel topographies were carried out with the laser-scanning microscope VK-X110 from the company Keyence. The optical scans of the topographies had a lateral resolution of app. 1 µm and a resolution in height of app. 0.005 µm. The measuring range of a single scan was limited to an area of 1 mm x 1 mm. The measurement of a bigger surface area was achieved by merging multiple scans using an implemented stitching-algorithm of the measurement software. The total measuring range of the investigated grinding wheel topographies were chosen so that the distribution of the grain shape characteristics reached a quasi-stationary state. For this purpose measurement plots of different length and width were analyzed. The results showed that a common measuring range of $L_{meas} = 7.5$ mm and $B_{meas} = 3.5$ mm is suitable to represent the investigated grinding wheel topographies. Since the identification of the kinematic cutting edges is based on kinematic-geometric engagement model developed by Weiß [12] a cut off area $A_{SA} = 10.5$ mm², corresponding to a cut off length $l_{SA} = 3$ mm, was defined at the front of the measurement plots in order to avoid distortion of the analysis results. Within this area the kinematic cutting edges are determined, but neglected for the analysis of the cutting edges. More and detailed information to this can be found in [12].

2.2. Analysis of the cutting edges

The analysis of the cutting edges is based on the grain shape characteristics opening angle α (horizontal in scratching direction), apex angle β (transversal to the scratching direction), rake angle γ and wedge angle δ (both in scratching direction) introduced by Rasim in [13], see Fig. 1.

In order to determine these grain shape characteristics of a single cutting edge, first its highest data point is identified (z-axis), representing the tip of the cutting edge. Subsequently, all data points of the cutting edge are identified, which are located in the same data line of the cutting edge tip in grinding direction (x-axis; Fig. 1 top-right) and crosswise (y-axis; Fig. 1 top-left). In the next step regression lines are determined starting from the tip of the cutting edge through the identified points, so that the apex angle β, the rake angle γ and the wedge angle δ are given by calculating the angle of intersection between the regression lines in x- and y-direction.

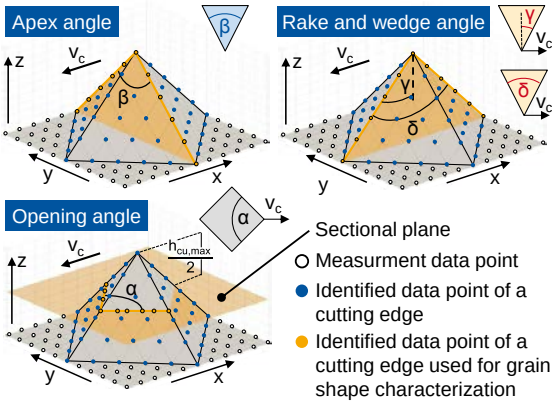

Fig. 1. Schematic illustration of the grain shape characteristics

To calculate the opening angle α first a sectional plane is shifted by the half of the maximum chip thickness $h_{cu,max}$ in normal direction below the tip of the cutting edge. Secondly, all intersection points of the cutting edge with the sectional plane are calculated. If a data line in x-direction has more than one intersection point, only the first intersection point in grinding direction is considered for the further calculations of the opening angle α. The maximum chip thickness $h_{cu,max}$ of a cutting edge is calculated from the maximum height distance between the tip and all data points lateral to the tip. At the next step, again two regression lines are determined starting from the foremost point of intersection through the other calculated intersection points. The opening angle α results analogously from the angle of intersection of the two regression lines.

2.3. Identification of kinematic cutting edges

The identification of the kinematic cutting edges of a topography measurement plot is based on kinematic-geometric engagement model developed by Weiß [12]. In his model the kinematic cutting edges are determined by using the limiting angle of cutting edge offset ε_{lim}, defined by Kassen and Werner, as geometric boundary condition of engagement [14,15]. The limiting angle of cutting edge offset ε_{lim} describes the kinematic shadowing effect of protruding abrasive grains on following grains as a function of the process parameters workpiece speed v_w, grinding wheel circumferential speed v_s, depth of cut a_e and grinding wheel diameter d_s and is given by

$$\tan \varepsilon_{lim} = \frac{v_w}{v_s} \cdot 2 \cdot \sqrt{\frac{a_e}{d_s}} \qquad (1)$$

The procedure of the identification of the cutting edges according to the model of Weiß is schematically shown in Fig. 2. As the figure illustrates, first within each data line in grinding direction all topography data points are identified, that fulfill the geometric boundary condition of engagement defined by the limiting angle of cutting edge offset ε_{lim}. After the identification of all data points that engage with the workpiece (kinematic data points), the resulting kinematic cutting edges are determined by grouping coherent kinematic data points to contiguous areas.

Hence, the model by Weiß identifies the cutting edges strictly using the limiting angle of cutting edge offset for engagement condition, only the influence of the process pa-

rameters v_w, v_s and a_e is considered. Thus an ideally-plastic workpiece material behaveior is presupposed. Elastic and plastic material deformations of the workpiece are neglected. Since the elastically deformed material springs back behind the cutting edge the actual machined material volume is smaller than that with an ideally-plastic material behavior. Consequently, taking elastic material deformations into account, the real shadowing effect of a grain is smaller than the kinematic shadowing effect.

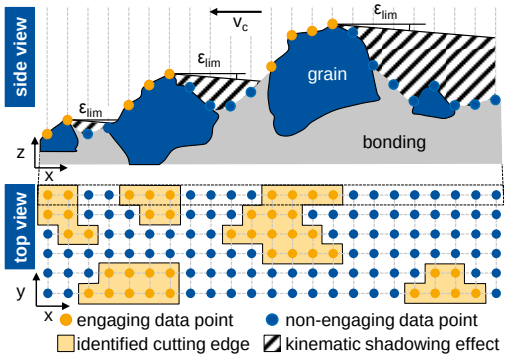

Fig. 2. Schematic illustration of the identification of cutting edges by Weiß

In addition to this, plastically deformed lateral elevations arise during the engagement of a grain with the workpiece (bulging). This causes that subsequent laterally offset grains penetrate stronger into the workpiece and thus the real shadowing effect is also decreased.

In order to better represent the material behavior of the workpiece, the kinematic-geometric engagement model by Weiß has been extended by the implementation of an elasto-plastic height offset Δh_{elpl}. The elasto-plastic height offset Δh_{elpl} reduces the kinematic shadowing effect by shifting the starting point of kinematic-geometric engagement boundary condition. Its functioning is schematically shown in Fig. 3.

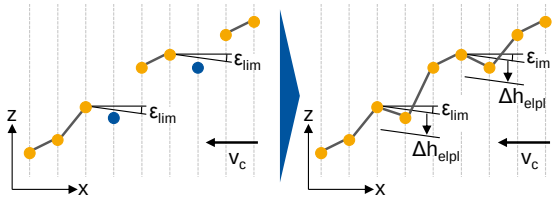

Fig. 3. Identification procedure of cutting edges with and without elasto-plastic higth offset Δh_{elpl}

The elasto-plastic height offset Δh_{elpl} consists of an elastic height offset Δh_{el}, taking the elastic material deformation of the workpiece into account, and a plastic height offset Δh_{pl}, representing the impact of bulging.

$$\Delta h_{elpl} = \Delta h_{el} + \Delta h_{pl} \tag{2}$$

The elastic height offset Δh_{el} corresponds to the specific plastic deformation depth T_{pl}, which is defined as the depth of cut when plastic deformations occur [13].

$$\Delta h_{el} = T_{pl} \tag{3}$$

The specific plastic deformation depth T_{pl} is determined according to the empirical approach in [13].

$$T_{pl} = c_\beta \cdot \beta + c_\delta \cdot \delta + c_{vc} \cdot v_c + c_S \cdot S + c_{const} \tag{4}$$

Within this equation the variable S describes the state of lubrication and can take values of S = 0 (no lubrication) and S = 1 (lubrication). The coefficients c_i are listed in the left column of Table 1 and have been experimentally examined by Rasim in [13] for a bearing steel 100Cr6 with a hardness of 60±1 HRC.

Table 1. Experimentally examined coefficients for T_{pl} and f_{ab}

Coefficient	Plastic Cutting Depth T_{pl}	Relative Chip Volume f_{ab}
c_α	---	0.000177
c_β	0.000952	-0.000214
c_γ	---	-0.000096
c_δ	0.000963	---
c_{vc}	0.00261	0.00141
c_S	0.00328	0.00426
c_{const}	-0.0851	0.9712

The plastically deformed elevations only occur beside the path of grain engagement and have an irregular height profile. For this reason the resulting reduction of the kinematic shadowing effect cannot be directly calculated from the elevations heights. Therefore the impact of plastically deformed lateral elevations has been approximated by an equivalent plastic height offset $\Delta h_{pl,eq}$, which represents the mean elevation height averaged over the effective grinding wheel width $b_{s,eff}$.

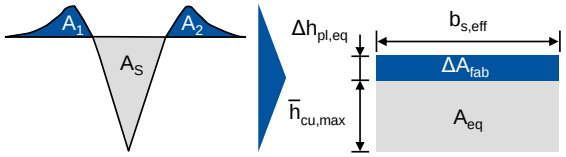

Fig. 4. Equivalent plastic height offset $\Delta h_{pl,eq}$ due to lateral elevations

In this context it is assumed, that the ratio of the elevations cross section area ($A_1 + A_2$) to the cross section area of the scratch path A_s complies with the ratio of the mean elevations height $\Delta h_{pl,eq}$ to the mean maximum chip thickness $\bar{h}_{cu,max}$ of all cutting edges. Since the ratio of the elevations cross section area ($A_1 + A_2$) to the cross section area of the scratch path A_s is given by the relative chip volume f_{ab}, the mean elevations height $\Delta h_{pl,eq}$ can be determined in the context of

$$1 - f_{ab} = \frac{A_1 + A_2}{A_S} = \frac{\Delta A_{fab}}{A_{eq}} = \frac{\Delta h_{pl,eq} \cdot b_{s,eff}}{\bar{h}_{cu,max} \cdot b_{s,eff}} = \frac{\Delta h_{pl,eq}}{\bar{h}_{cu,max}} . \tag{5}$$

The relative chip volume f_{ab} can be defined based on findings in [16,17] or analogously to Eq. 4 by an empirical approach using the single grain scratching method by Rasim. The latter method was used in this publication, leading to Eq. 6 [18]. The coefficients c_i, experimental examined for bearing steel 100Cr6 with a hardness of 60±1 HRC, are listed in right column of Table 1.

$$f_{ab} = c_\alpha \cdot \alpha + c_\beta \cdot \beta + c_\gamma \cdot \gamma + c_{vc} \cdot v_c + c_S \cdot S + c_{const} \tag{6}$$

As the shape of the elevations is not known and thus it cannot be clearly assigned which grain comes into engagement with the elevations of a leading grain, the elasto-plastic height offset and its influence on the kinematic shadowing effect cannot be determined for each grain. Therefore, an averaged elasto-plastic height offset $\overline{\Delta h_{elpl}}$ is used for the total topography analysis. It is calculated by the average plastic cutting depth $\overline{T}_{pl}$ and the mean relative chip volume $\bar{f}_{ab}$ of all cutting edges.

$$\overline{\Delta h}_{elpl} = \overline{T}_{pl} + \Delta h_{pl,eq} = \overline{T}_{pl} + \overline{h}_{cu,max} \cdot (1 - f_{ab}) \quad (7)$$

Eq. 4 and 6 show, that the grain shape characteristics of the cutting edges are used for identifying the cutting edges. Since the grain shape characteristics themselves depend on the identified cutting edges, an iterative procedure was chosen. Firstly, the cutting edges are determined without elasto-plastic height offset. Subsequently, the grain shape characteristics are analyzed. Based on the determined grain shape characteristics the averaged elasto-plastic height offset is calculated. Finally the identification of the cutting edges with elasto-plastic height offset is performed.

The described procedure is based on the assumption that additional engaging grains, which appear due to the reduction of shadowing by the elasto-plastic height offset, create no further plastic elevations, since an already elevated workpiece material has a reduced deformability due to hardening processes and therefore shears directly. Consequently, the additional engaging grains have no influence on the elasto-plastic height offset, so that a topography analysis, run with one height offset iteration-loop, already leads to stable results.

3. Results and Discussion

In order to analyze the grinding wheel topography with the elasto-plastic grain engagement model, three single-layered, electroplated CBN grinding wheels were investigated with the same process parameters. The variation of the grinding wheel was performed on the mean grain size (151 µm/213 µm) and the grain type (ABN300/ABN900 from Element Six), see Table 2.

Table 2. Variation of the investigated CBN grinding wheel

Grain Specification	Grain Type	Dimension d_s x b_s
B213	ABN900	400 mm x 15 mm
B213	ABN300	400 mm x 15 mm
B151	ABN300	400 mm x 15 mm

The experimental grinding investigations were carried out with process parameter combinations that vary relating to the cutting speed v_c and to the limiting angle of cutting edge offset ε_{lim}. The cutting speed v_c was varied in the range of 10-60 m/s. The speed ratio was at q > 2000 for all investigations, so that the cutting speed v_c and circumferential grinding wheel speed v_s were taken equal. Through this the limiting angle of cutting edge offset ε_{lim} could be kept constant at the variation of cutting speed v_c on appropriate choice of constant speed ratio q. The variation of the limiting angle of cutting edge offset ε_{lim} at constant cutting speed v_c was performed by a variation of the specific material removal rate Q'_w in the range of 5-30 mm³/mms and a depth of cut a_e of 1 mm and 2 mm. The used plan of investigation is summarized in Fig. 5.

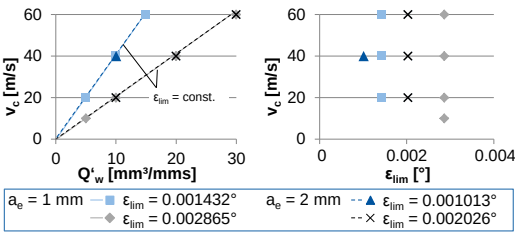

Fig. 5. Investigated process parameters

In order to draw conclusions from the grinding wheel topography analysis to the energy conversion in grinding, at all investigation points the process force on the workpiece, locally dissolved along the contact length, was measured using the developed setup by Duscha [19].

To establish comparability between the topography analysis results the grain shape characteristics α, β and γ as well as the maximum chip thickness $h_{cu,max}$ of the cutting edges have been binned into equidistant classes and the relative frequency for each class has been calculated.

Fig. 6 shows the comparison of the topography analysis result of the two investigated grinding wheels with different grain types (ABN300 vs. ABN900), same mean grain size (B213) at the same process parameter combination. The number of the kinematic cutting edges N_{kin} of both grinding wheel topographies correlates with the identified values by Weiß for vitrified CBN grinding wheels [12]. Also Yegenoglu determined values for the number of kinematic cutting edges of this scale in his findings in [20]. As the figure shows, the variation of grain type led only to minor differences in the number of kinematic cutting edges N_{kin}. In contrast to this, the influence of the grain type on the frequency distributions of the grain shape characteristics is obviously. In particular, the rake angle and the apex angle frequency distributions of the grinding wheel with grain type ABN900 have a more equal distribution compared to the distributions of the grinding wheel with grain type ABN300. This is due to the greater variation of the grain morphology of ABN900.

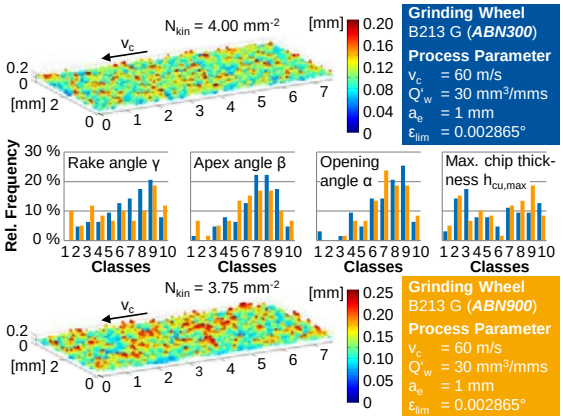

Fig. 6. Influence of the grain type on the grain shape characteristics

Fig. 7 illustrates the results of the topography analysis of the two investigated grinding wheels with different mean grain size (B151 vs. B213) and the same grain type (ABN300). The smaller grain size led to a greater number of kinematic cutting edges and to smaller maximum chip thicknesses. The grain size had no significant influence on the distributions of grain shape characteristics. Due to the same process parameter combination and thus the same limiting angle of cutting edge off set ε_{lim}, the results confirm, that the grain morphology of both grinding wheel variants were the same and independent of the grain size.

Fig. 8 shows the experimentally determined tangential force curves of the three investigated grinding wheel variations at same process parameter combination. The grinding wheel variant with grain type ABN900 and a mean grain size

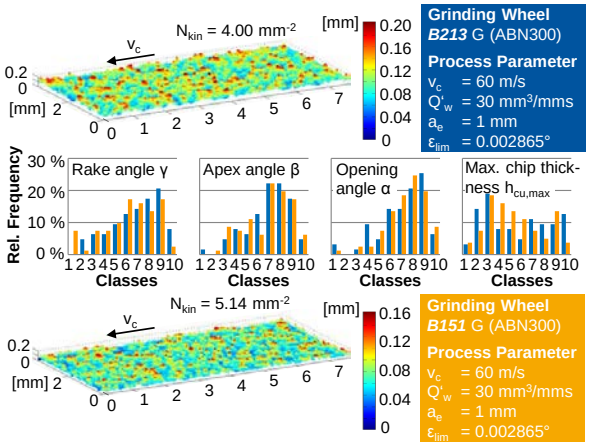

Fig. 7. Influence of the grain size on the grain shape characteristics

of 213 µm shows the lowest tangential force curve. This can be attributed to the differences in the probability distributions of the grain shape characteristics which results from larger variance of the grain morphology (see Fig. 6). In particular, the smaller negative rake angles of grain type ABN900 compared to ABN300 led to an earlier occurrence of plastic deformations and chip formation [13], to smaller normal grain contact surfaces and thus less energy was converted. The grinding wheel variant with grain type ABN300 and a mean grain size of 151 µm led to the curve with the highest tangential forces. As shown in Fig. 7 grinding wheels with same grain type at the same process parameter combination led to similar distributions of the grain shape characteristics and maximum chip thickness. Thus, the higher forces result due to a higher number of kinematic cutting edges.

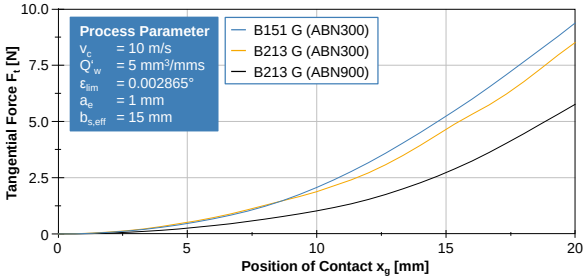

Fig. 8. Comparison of tangential force curves with varying grinding wheels

The comparison of the tangential force curves of all three grinding wheels variants shows, that at the present process parameter combination the shape of the cutting edges has a significantly stronger impact on the energy conversion than the number of kinematic cutting edges N_{kin}.

Overall, the results show that the influence of the grinding wheel topography on the energy conversion can be registered qualitatively by the developed kinematic-geometric engagement model. Thus, the presented approach of the geometric characterization of grinding wheel topographies can be used to find new or to improve existing modelling approaches of energy conversion in grinding.

In further investigations an energy model will be developed, which determines the energy conversion during the single-grain cut in dependency of the grain shape characteristics. This model will be transferred from the energy conversion of the single-grain cut to the multi-grain cut of a grinding wheel using analysis results of the presented kinematic-geometric engagement model.

Acknowledgements

The authors would like to thank the German Research Foundation (DFG) for the support of the depicted research within the project SFB/TR 96-A03.

References

[1] Tönshoff HK, Peters J, Inasaki I, Paul T. Modelling and Simulation of Grinding Processes. In: CIRP Annals; 1992;41(2):677-88.
[2] Malkin S, Guo C. Grinding Technology: Theory and Applications of Machining with Abrasives. 2nd ed. NY:Industrial Press; 2008. pp. 121 ff.
[3] Rowe WB. Principles of Modern Grinding Technology. 1st ed. Oxford: William Andrew; 2009. p. 334 f.
[4] Ghosh S, Chattopadhyay AB, Paul S. Modelling of specific energy requirement during high-efficiency deep grinding. In: International Journal of Machine Tools and Manufacture; 2008;48(11):1242-53.
[5] Singh V, Venkateswara Rao P, Ghosh S. Development of specific grinding energy model. In: International Journal of Machine Tools and Manufacture; 2012;60:1-13.
[6] Badger JA, Torrance AA. A comparison of two models to predict grinding forces from wheel surface topography. In: International Journal of Machine Tools and Manufacture; 2000;40(8):1099-120.
[7] Holtermann R, Schumann S, Menzel A, Biermann D. Modelling, simulation and experimental investigation of chip formation in internal traverse grinding. In: Prod. Eng. Res. Devel.; 2013;7:251-63.
[8] Holtermann R, Menzel A, Schumann S, Biermann D, Siebrecht T, Kersting P. Modelling and simulation of Internal Traverse Grinding: bridging meso- and macro-scale simulations. In: Prod. Eng. Res. Devel.; 2015;9:451-63.
[9] Görne J. Simulationsmodell zur Prozeßauslegung beim Schrägeinstechschleifen. Dissertation RWTH Aachen; 1986. p. 80 ff.
[10] Chang HC, Junz Wang JJ. A stochastic grinding force model considering random grit distribution. In: International Journal of Machine Tools and Manufacture; 2008. No. 48/12-13. p. 1335-44.
[11] Hecker RL, Liang SY, Wu XJ, Xia P, Jin DGW. Grinding force and power modeling based on chip thickness analysis. In: International Journal of Advanced Manufacturing Technologies; 2007;33:449-59.
[12] Weiß M, Klocke F, Barth S, Rasim M, Mattfeld P. Detailed Analysis and Description of Grinding Wheel Topographies. In: Proceedings of the ASME; 2015; MSEC2015. June 8-12. Charlotte. North Carolina. USA.
[13] Rasim M, Mattfeld P, Klocke F. Analysis of the grain shape influence on the chip formation in grinding. In: Journal of Materials Processing Technology; 2015;226:60-8.
[14] Kassen G, Werner G, Kinematische Kenngrößen des Schleifvorganges. In: Industrieanzeiger; 1969;91(87):2087-90.
[15] Werner G. Kinematik und Mechanik des Schleifprozesses. Dissertation RWTH Aachen; 1971. p. 46 ff.
[16] Giwerzew A. Spanbildungsmechanismen und tribologisches Prozessverhalten beim Schleifen mit niedrigen Schnittgeschwindigkeiten. Dissertation Universität Bremen; 2003.
[17] Martin K, Yegenoglu K. HSG-Technologie - Handbuch zur praktischen Anwendung. Guehring Automation GmbH; 1992.
[18] Rasim M. Modellierung der Wärmeentstehung im Schleifprozess in Abhängigkeit von der Schleifscheibentopographie. Dissertation RWTH Aachen; 2016.
[19] Duscha M. Beschreibung des Eigenspannungszustandes beim Pendel- und Schnellhubschleifen. Dissertation RWTH Aachen; 2014.
[20] Yegenoglu K. Berechnung von Topographiekenngrößen zur Auslegung von CBN-Schleifprozessen. Dissertation RWTH Aachen; 1986. p. 61.